Online Walking Pattern Generation for Biped Humanoid Robot with Trunk.

Conference Paper · January 2002

DOI: 10.1109/ROBOT.2002.1013705 · Source: DBLP

3 authors, including:

Hun-ok Lim
Kanagawa University

Atsuo Takanishi
Waseda University

Proceedings of the 2002 IEEE
International Conference on Robotics & Automation
Washington, DC • May 2002

Online Walking Pattern Generation for Biped Humanoid Robot with Trunk

Hun-ok Lim*†, Yoshiharu Kaneshima‡ and Atsuo Takanishi*†

*Department of System Design Engineering, Kanagawa Institute of Technology
1030 Shimoogino, Atsugi, Kanagawa, 243-0292 Japan
Tel/Fax:81-46-291-3266, E-mail: holim@sd.kanagawa-it.ac.jp
‡Ishikawajima-Harima Heavy Industry Co., Ltd.
*Department of Mechanical Engineering, Waseda University
†Humanoid Robotics Institute, Waseda University

Abstract

This paper describes an online method generating walking patterns for biped humanoid robots having a trunk. Depending on the walking command, the motion patterns of the lower-limbs are created and connected to the prewalking patterns smoothly in online. For the stability of the biped robots, the trunk and the waist motion is generated by a walking stabilization control that is based on the ZMP trajectory and the motion of the lower-limbs. Experimental tests of versatile biped walking on a plane surface are conducted using an auditory interface, and the validity of the online pattern generation method is verified.

1. Introduction

Biped humanoid robots are expected to be used not only into industrial areas, but also into non-industrial areas, such as to services in homes and offices and for social welfare. To date, we have studied biped-walking motion with two main thrusts to apply the biped robots to the fields. One trust has been toward realizing dynamic complete walking on not only even or uneven terrain but also hard or soft terrain. In 1973, we developed WABOT-1 that consists of a torso, a perceptual system and two artificial arms and legs, and realized the static walking on a horizontal plane [1]. Moreover, we realized the dynamic complete walking on even or uneven terrain using WL series [2]. The other thrust has been toward exploring human-robot interaction and real-time walking. The dynamic biped walking was achieved under the unknown external forces applied by an environment [3]. Also, the emotional motion of the biped robot was presented which is expressed by the parameterization of its body motion [4].

Other research groups have studied on walking control and energy consumption [5, 6, 7, 8, 9]. Vukobratovic and his co-workers modeled the walking biped robot that balances by manipulating the projected center of gravity and the support area provided by the feet [10]. Honda's humanoid robot called P3 has been constructed and realized dynamic walking on a plane and a stairway [11]. Until now, almost all biped-walking has been realized by the offline pattern generation. Many researchers studied these offline pattern generation [12, 13, 14, 15, 16]. In order to coexist with humans, a walking pattern should be generated in real-time according to a human-living environment. Then, it goes without saying that the visual and the auditory information are necessary to make a walking pattern reliable at the environment. However, the real-time pattern generation for biped humanoid robots has not been reported so much.

In this paper, how to generate continuous walking patterns in online is proposed. The pattern generation consistes of two parts such as a lower-limb motion and an upper-body motion. As soon as the biped robot begins walking, the pattern of the lower-limb is generated from three steps to five steps according to the walking parameters. At the same time, the pattern of the upper body is determined by a walking stabilization control method, which is employed to compensate for moments generated by the motion of the lower-limbs. Here, the walking parameters can be set by the auditory and visual information.

This paper is organized as follows. In section 2, we describe online walking pattern generation. Section 3 describes a stabilization control to cancel the produced moments. Section 4 illustrates experimental systems and shows experimental results. Finally, Section 5 provides conclusions.

2. Online pattern Generation

2.1 Coordinate Frames

A 43-DOF biped model with rotational joints is considered in this study, which consists of two 6-DOF legs, two 7-DOF arms, two 3-DOF hands, a 4-DOF neck, two 2-DOF eyes and a torso with a 3-DOF waist. To define mathematical quantities, a world coordinate frame $\mathcal{F}$ is fixed on the floor where the biped robot can walk and a moving coordinate frame $\bar{\mathcal{F}}$ is attached on the center of the waist to consider the relative motion of each particle (see Figure 1). In modeling, five assumptions are defined as follows:
(1) The biped robot consists of a set of particles,
(2) The foothold of the biped robot is rigid and not moved by any force and moment,
(3) The contact region between the foot and the floor surface is a set of contact points,
(4) The coefficients of friction for rotation around the X, Y and Z-axes are nearly zero at the contact point between the feet and the floor surface and
(5) The feet of the robot do not slide on the contact surface.

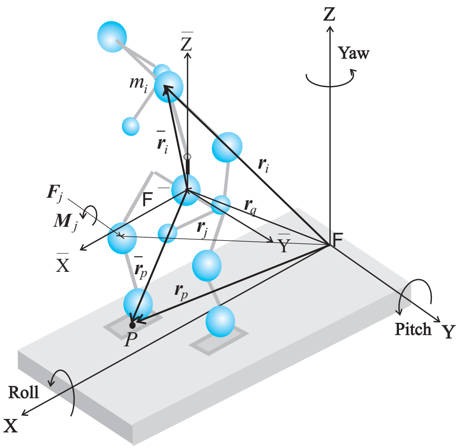

Figure 1: Coordinate frames

2.2 Walking Pattern Generation

A walking cycle consists of five phases as shown in Figure 2: stationary, transient, steady, transient and stationary phases. The transient phase is a step after or before the stationary phase because the dynamics of the upper-body shoud be considered for stability (see Section 3). An online pattern generator makes a continuous walking pattern as shown in Figure 3. First, walking parameters are inputted to the pattern generator, which are a step length, step height and step direction determined by the visual and auditory information and so on. Second, The pattern generator makes a five-step pattern of the lower-limb and sets a target ZMP pattern in the stable polygon. Third, the compensatory motion of the trunk and the waist is calculated from the trajectories of the lower-limb and the ZMP by using the walking motion control method. Finally, the middle step of the five-step pattern and the compensatory motion pattern is selected for a next step and is held to the first step of the pattern generator to make a future step.

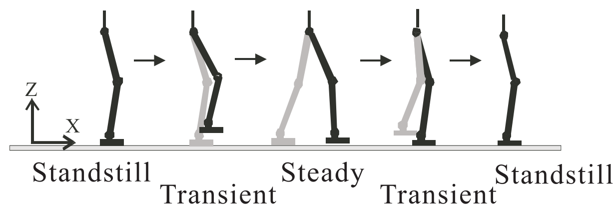

Figure 2: A walking cycle

We here describe how to determine the pattern of the lower-limb more in detail as follows:
(a) Five steps are made in real-time as soon as the biped humanoid robot begins walking. The pattern generator selects from the first step to the third step.
(b) On the third step, three steps (from the fourth step to the fifth step) are generated to satisfy the dynamic conditions of the second and the third lower-limb step. The fourth step is chosen.
(c) On the fourth step, three steps (from the fifth step to the seventh step) are generated to satisfy the dynamic conditions of the third and the fourth lower-limb step. The fifth, sixth and seventh step are selected.
(d) A continuous walking pattern is generated in online, repeating the above procedure. Figure 4 shows the pattern generation of the lower-limb.

A continuous walking pattern is simulated which is generated by the online pattern generator. The forward step is changed to the backward step at 17 sec. Figure 5 shows the pitch trajectories of the thigh. We can see that the connection between the forward and the backward steps is not rough.

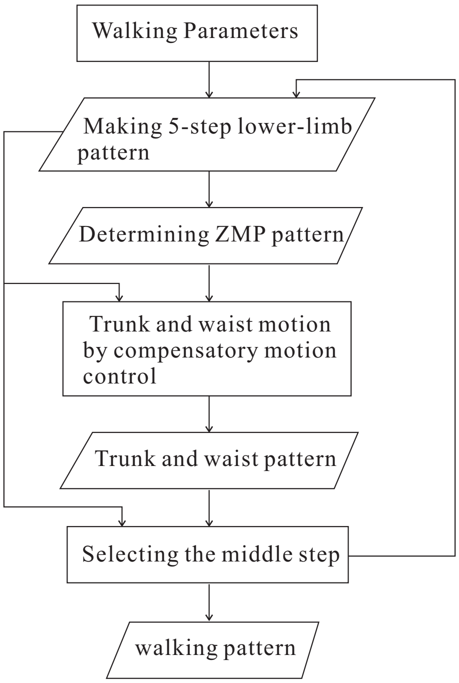

Figure 3: Online pattern generation

3. Walking Stabilization Control

3.1 ZMP Equation

Under the modeling assumptions, the moment balance around a contact point p between the foot and the ground with respect to the world coordinate frame can be written as

$$\sum_{j=1}^{n}((\boldsymbol{r}_j - \boldsymbol{r}_p) \times \boldsymbol{F}_j + \boldsymbol{M}_j)$$
$$-\sum_{i=1}^{n} m_i(\boldsymbol{r}_i - \boldsymbol{r}_p) \times (\ddot{\boldsymbol{r}}_i + \boldsymbol{G}) = \boldsymbol{T} \qquad (1)$$

where $\boldsymbol{r}_p$ is the position vector of the point p from the origin of $\mathcal{F}$. m_i is the mass of the particle i. $\boldsymbol{r}_i$ and $\ddot{\boldsymbol{r}}_i$ denote the position and acceleration vectors of the particle i with respect to the world coordinate frame $\mathcal{F}$, respectively. $\boldsymbol{G}$ is the gravitational acceleration vector. $\boldsymbol{T}$ is the moment vector acting on the contact point p. $\boldsymbol{r}_j$ denotes the position vector of the particle j with respect to the world coordinate frame $\mathcal{F}$. $\boldsymbol{F}_j$ and $\boldsymbol{M}_j$ denote the force and the moment vectors acting on the particle j relative to the frame $\mathcal{F}$, respectively.

Let ZMP be on the point p. The moment $\boldsymbol{T}$ is zero according to the ZMP concept. To get the relative

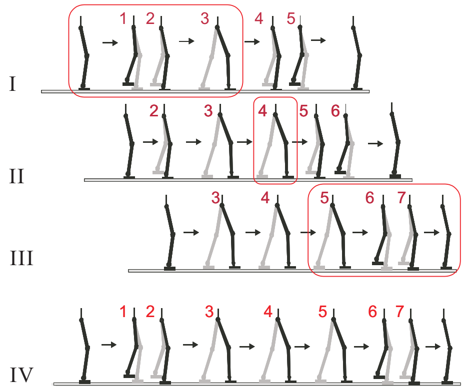

Figure 4: Lower-limb's pattern generation

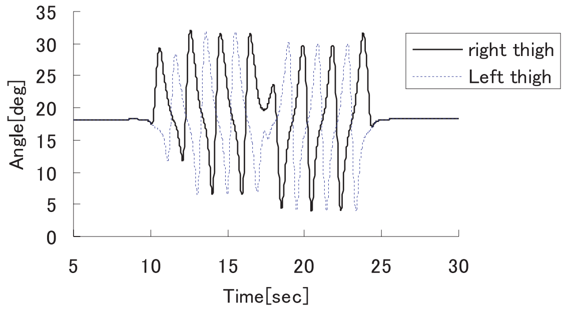

Figure 5: Step change simulation

motion of particles, Equation (1) is changed relative to the moving frame $\bar{\mathcal{F}}$ as follows:

$$\sum_{i=1}^{n} m_i(\bar{\boldsymbol{r}}_i - \bar{\boldsymbol{r}}_{zmp}) \times (\ddot{\bar{\boldsymbol{r}}}_i + \ddot{\boldsymbol{r}}_q + \boldsymbol{G}$$
$$+\dot{\bar{\boldsymbol{\omega}}} \times \bar{\boldsymbol{r}}_i + 2\bar{\boldsymbol{\omega}} \times \dot{\bar{\boldsymbol{r}}}_i + \bar{\boldsymbol{\omega}} \times (\bar{\boldsymbol{\omega}} \times \bar{\boldsymbol{r}}_i))$$
$$-\sum_{j=1}^{n}((\bar{\boldsymbol{r}}_j - \bar{\boldsymbol{r}}_{zmp}) \times \bar{\boldsymbol{F}}_j + \bar{\boldsymbol{M}}_j) = \boldsymbol{0}, \qquad (2)$$

where $\bar{\boldsymbol{r}}_{zmp}$ is the position vector of ZMP with respect to the $\bar{\mathcal{F}}$. $\boldsymbol{r}_q$ is the position vector of the origin of the frame $\bar{\mathcal{F}}$ from the origin of the frame $\mathcal{F}$. $\bar{\boldsymbol{\omega}}$ and $\dot{\bar{\boldsymbol{\omega}}}$ denote the angular velocity and acceleration vectors, respectively.

Equation (2) is non-linear because the three-axis motion of the trunk is interferential each other. It, therefore, is difficult to derive analytic solutions of the trunk and the waist. We assume that (a) the external forces are not considered in the approximate model,

(b) the upper body is modeled as a four-mass model, (c) the moving frame does not rotate, (d) the trunk and the waist do not move vertically, and (e) the trunk arm rotates on the horizontal plane only.

The moment generated by the lower-limb's motion is periodic functions because each particle of the lower-limbs and the time trajectory of ZMP move periodically with respect to the moving frame $\bar{\mathcal{F}}$. Therefore, the equation can be represented as a Fourier series. Comparing the Fourier transform coefficients of the components of the lower-limb and the upper body, the approximate periodic solutions of the pitch and the roll trunk and waist can be obtained. By regarding a complete walking as one walking cycle and making static standing states before and after walking long enough, the approximate solutions of the compensatory trunk and waist for the complete walking can be derived. Also, the strict solutions of the trunk and the waist motion can be obtained by a recursive method [4].

3.2 Motion of Upper Body

When the gait of the lower-limb is changed dynamically according to human's living/working environments, the dynamics of the trunk and the waist motion should be considered to compensate for the moments generated by the lower-limb motion. Assuming that the waist is immovable, the pitch and the roll moment components of Equation (2) can be changed as

$$(\bar{z}_t - \bar{z}_{zmp})\ddot{\bar{x}}_t - g_z\bar{x}_t = A(t), \tag{3}$$

$$(\bar{z}_t - \bar{z}_{zmp})\ddot{\bar{y}}_t - g_z\bar{y}_t = B(t), \tag{4}$$

where

$$A(t) = \frac{M_y(t) - m_w(\bar{z}_w - \bar{z}_{zmp})\ddot{\bar{x}}_w + m_w g_z \bar{x}_w}{m_t},$$
$$B(t) = \frac{-M_x(t) - m_w(\bar{z}_w - \bar{z}_{zmp})\ddot{\bar{y}}_w + m_w g_z \bar{y}_w}{m_t}, \tag{5}$$

M_y and M_x denote the pitch and the roll moments generated by the motion of the lower-limb, respectively.

Consider only the motion of the trunk around the pitch axis to investigate the compensatory motion. The transfer function in the frequency domain between the trunk motion $B(t)$ and $\bar{y}_t$, $y(\omega)$, can be expressed as

$$y(\omega) = \frac{2p}{\omega^2 + p^2}q = (\frac{1}{p - j\omega} + \frac{1}{p + j\omega})q, \tag{6}$$

where

$$p = \sqrt{\frac{g_z}{\bar{z}_t - \bar{z}_{zmp}}}, \quad q = -\frac{1}{2g_z}\sqrt{\frac{g_z}{\bar{z}_t - \bar{z}_{zmp}}}. \tag{7}$$

According to the ZMP concept, $\bar{z}_{zmp}$ in Equation (7) is zero. Equation (6) is generally known as Lorentz function, and its primitive function is written as

$$y(t) = qe^{-p|t|}. \tag{8}$$

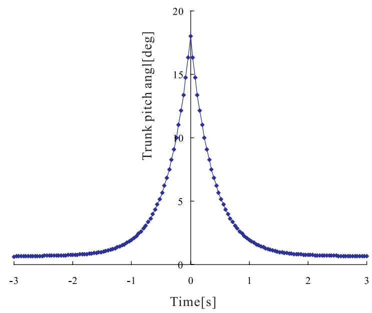

Figure 6: Compensatory motion of the trunk.

We can imagine from Equation (8) that the casual law may not be applied anymore. If the walking speed of the biped robot is increased more, it goes without saying that $y(t)$ affects stability more badly. The trunk, therefore, should be in motion earlier than the shift of ZMP to cancel the effect of the produced moments. The relationship between the trunk motion and the applied force has been simulated. When a biped robot is not in motion, an impulse moment 1000 Nm is applied to the pitch trunk. Figure 6 shows the pitch motion of the trunk. In this simulation, we can see that the compensatory motion of the trunk should be begun with a view of balancing before and after the impulse moment is applied to the biped robot.

4. Experimental Tests

4.1 Motor and Auditory Systems

To explore follow-walking motion, a forty-three mechanical degrees of freedom WABIAN-RIV with a human configuration has been constructed. Its height is about 1.89 m and its total weight is 131.4 kg. Duralumin, GIGAS (YKK Corporation) and CFRP (Carbon Fiber Reinforced Plastic) are mainly employed as structural materials. The body and legs are driven by AC servo motors with reduction gears. The neck, hands and arms are actuated by DC servo motors with reduction gears, but the eyes by DC servo motors without reduction gears.

IMB's ViaVoice system is used as a voice recognition engine. In this study, we let the voice system to respond to only the preset voice vocabularies. There are eight voice commands. The step length as a walking parameter is defined by compiling the text file of Grammar Control. Table 1 shows the step length with regard to the specialized vocabularies.

Table 1: Voice Command.

Voice	SP m	LP m	Turning deg
Forward	0.10	0.00	0.00
Backward	-0.10	0.00	0.00
Right	0.00	-0.05	0.00
Left	0.00	0.05	0.00
Right turning	None	None	-5.00
Left Turning	None	None	5.00
Standstill	0.00	0.00	0.00
Stop	None	None	None

SP: Sagittal Plane
LP: Lateral Plane

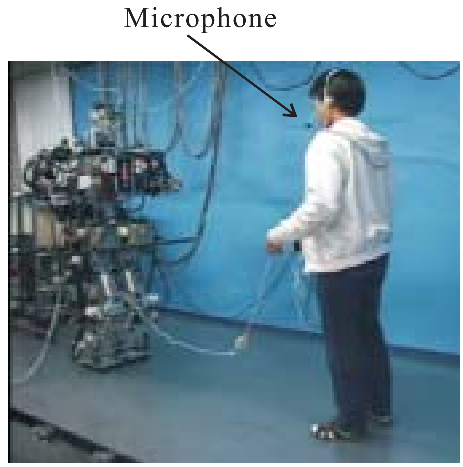

Figure 7: Walking experiment by voice

4.2 Experimental Results

Figure 7 shows a scene of the walking experiment conducted by the auditory sensing. The continuous dynamic walking on a flat plane is realized with the step time of 0.96 s/step, the forth-and-back step length of 0.1 m/step, the side step length of 0.05 m/step and the turning angle of 5 deg/step. Figure 8 shows the sagittal ZMP trajectory measured by a force/torque sensor. The measured maximum and minimum ZMP is about 160 mm and -170 mm respectively, while WABIAN-RIV is able to maintain the maximum and minimum ZMP of 240 mm and -240 mm, respectively. This tells us that the proposed pattern generation and walking control is useful for real-time dynamic walking.

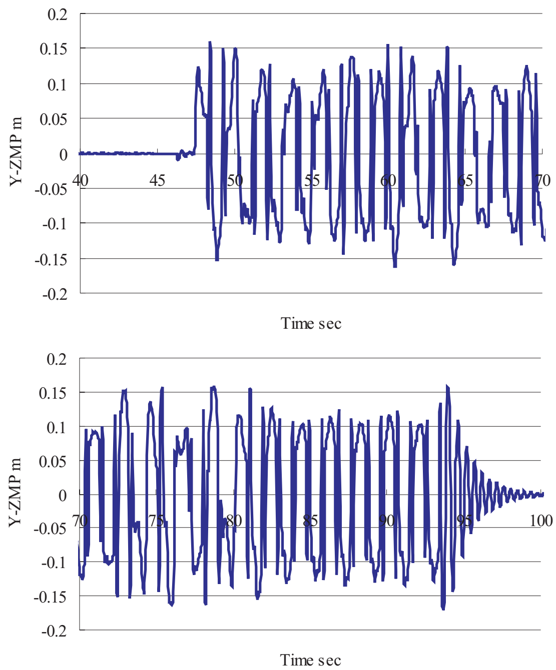

Figure 8: ZMP trajectory in sagittal plane

5. Conclusion

An online pattern generation is presented to achieve continuous dynamic walking. In making a walking pattern, walking parameters are firstly determined through human-robot interface using visual and auditory sensors. The pattern generator and control method generate the complete pattern that consists of patterns of the lower-limb and the upper body. The upper-body motion compensates for the moments produced by the motion of the lower-limb and follows the desired ZMP trajectory set in the stable polygon. Versatile walking on a plane surface is conducted using an auditory and a visual interface, and the effectiveness of the pattern generation method is verified.

Acknowledgment

This study has been conducted as a part of the humanoid project at Humanoid Robotics Institute, Waseda University. This study was funded in part by JSPS (Japan Society for the Promotion of Science) under Japanese Grant-in-Aid for Scientific Research and NEDO (New Energy and Industrial Technology Development Organization). The authors would like to thank Okino Industries Ltd., Harmonic Drive Systems Inc. and YKK Corporation for supporting us in developing the hardware.

References

[1] I. Kato, S. Ohteru, H. Kobayashi, K. Shirai, and A. Uchiyama, "Information-power machine with senses and limbs," in *Proc. CISM-IFToMM Symp. Theory and Practice of Robots and Manipulators*, Udine, Italy, Sep. 1973, pp. 12–24.

[2] A. Takanishi, H. O. Lim, M. Tsuda, and I. Kato, "Realization of dynamic biped walking stabilized by trunk motion on a sagitally uneven surface," in *Proc. IEEE/RSJ Int. Workshop Intelligent Robots and Systems*, Tsuchiura, Japan, Jul. 1990, pp. 323–329.

[3] A. Takanishi, T. Takeya, H. Karaki, M. Kumeta, and I. Kato, "A control method for dynamic walking under unknown external force," in *Proc. IEEE/RSJ Int. Workshop Intelligent Robots and Systems*, Tsuchiura, Japan, Jul. 1990, pp. 795–801.

[4] H. O. Lim, A. Ishii, and A. Takanishi, "Motion pattern generation for emotion expression," in *Proc. Int. Symp. Humanoid Robots*, Tokyo, Japan, Oct. 1999, pp. 36–41.

[5] H. Benbrahim and J.A. Franklin, "Biped dynamic walking using reinforcement learning," *Robotics and Autonomous Systems*, vol. 22, pp. 238–302, 1997.

[6] J.A. Golden and Y.F. Zheng, "Gait synthesis for the as-2 biped robot to climb stairs," *Int. J. Robotics and Automation*, vol. 5, no. 4, pp. 149–159, 1990.

[7] Y. Hurmuzlu, "Dynamics of bipedal gait: part i-objective functions and the contact event of a planar five-link biped," *J. of Applied Mechanics*, vol. 60, pp. 331–336, 1993.

[8] R. Katoh and M. Mori, "Control method of biped locomotion giving asymptotic stability of trajectory," *Automatica*, vol. 20, no. 4, pp. 405–414, 1984.

[9] Shuuji Kajita, Tomio Yamaura, and Akira Kobayashi, "Danamic walking control of a biped robot along a potential energy conserving orbit," vol. 6, no. 1, pp. 431–438, 1992.

[10] M. Vukobratovic, A. A. Frank, and D. Juricic, "On the stability of biped locomotion," *IEEE Trans. of Biomedical Engineering*, vol. 17, no. 1, pp. 25–36, 1970.

[11] K. Hirai, M. Hirose, Y. Haikawa, and T. Takenaka, "The development of honda humanoid robot," in *Proc. IEEE Int. Conf. Robotics and Automation*, Leuven, Belgium, May 1998, pp. 1321–1326.

[12] F. M. Silva and J. A. Machado, "Towards efficient biped robots," in *Proc. IEEE/RSJ Int. Conf. Intelligent Robots and Systems*, 1998, pp. 394–399.

[13] C. Chevallereau, A. Formal, and B. Perrin, "Low energy cost reference trajectories for a biped robot," in *Proc. IEEE Int. Conf. Robotics and Automation*, Leuven, Belgium, May 1998, pp. 1398–1404.

[14] L. Roussel, C. Canudas de Wit, and A. Goswami, "Generation of energy optimal complete gait cycles for biped robot," in *Proc. IEEE Int. Conf. Robotics and Automation*, Leuven, Belgium, May 1998, pp. 2036–2041.

[15] M. Rostami and G. Bessonnet, "Impactless saggittal gait of a biped robot during the single support phase," in *Proc. IEEE Int. Conf. Robotics and Automation*, Leuven, Belgium, May 1998, pp. 1385–1391.

[16] P.H. Channon, S.H. Hopkins, and D.T. Phan, "Derivation of optimal walking motions for a biped walking robot," *Robotica*, vol. 10, no. 2, pp. 165–172, 1992.